Imaging of $c(8\times2)/(4\times6)$ GaAs(001) surface with noncontact atomic force microscopy

J. J. Kolodziej,* B. Such, and M. Szymonski
Marian Smoluchowski Institute of Physics, Jagiellonian University, Reymonta 4, 30-059 Kraków, Poland
(Received 1 October 2004; revised manuscript received 29 November 2004; published 15 April 2005)

Noncontact atomic force microscopy is used to study GaAs(001) surface having the $c(8\times2)/(4\times6)$ reconstruction, which is often found for surfaces prepared at temperatures close to 900 K. Images taken with large tip-surface separations show hazy features, so-called ghosts X, aligned in chains parallel to the $\langle\bar{1}10\rangle$ direction and partially disordered but tending towards $(\times6)$ period along $\langle110\rangle$. However, at lower tip-surface separation only a (4×1) pattern is clearly visible due to resolved surface atomic structure. The atomic-scale images are consistent with the recently proposed ζ model of $c(8\times2)$ reconstructed $A_{III}B_V$ surfaces. Those findings indicate that the ghosts are visualized through modulation of the electric field only, and consequently they are of electronic but not structural origin.

DOI: 10.1103/PhysRevB.71.165419 PACS number(s): 68.35.Bs, 68.37.Ps, 68.47.Fg, 73.20.−r

I. INTRODUCTION

Surface structures are widely studied not only because of the intellectual challenge but because surface properties are critical in many contemporary device technologies. An example of a technologically important surface is GaAs(001), often used as a substrate for molecular beam epitaxy (MBE)-grown electronic, optoelectronic, and magnetic devices. That surface is of complex nature and exposes many different reconstructions depending on stoichiometry of the top bilayer. Recent efforts of several research groups[1–4] have led to the establishment of a reliable model of the $c(8\times2)$ reconstructed (001) surfaces of $A_{III}B_V$ compounds. However, the $c(8\times2)$ GaAs surface, which is obtained after processing at temperatures 850–900 K and at low-arsenic conditions, as a rule has "admixed" (4×6) symmetry. Xu *et al.*,[5] based on scanning tunneling microscopy (STM) experiments, have suggested that there exists a single Ga-rich phase, called genuine (4×6) [or G(4×6)], which arises due to additional features (clusters of six to eight Ga atoms) distributed on regular (4×6) superlattice over (4×2).[6] The same authors reported also a disordered (4×6) surface, of basic construction similar to the G(4×6) one, but the additional features are not fully regularly distributed and form "meandering wormlike structures." Other authors who recently studied Ga-rich GaAs surfaces prepared at temperatures in the range of 850–900 K using either molecular beam epitaxy or ion sputtering have only found the disordered (4×6) phase; cf. papers by Kruse *et al.*,[7] Moosbuehler *et al.*,[8] and Negoro *et al.*[9] Most probably, there is indeed no qualitative difference between the G(4×6) phase and the disordered (4×6) phase since the strict order in images of G(4×6) surface published by Xu *et al.* is seen only locally[5,10] and, on the other hand, in the disordered phase one can often find almost regular parts.[5,7,8] Alternative explanation of the surface structure under discussion, also based on STM data, was suggested by Kruse *et al.*, who proposed that the visible bright spots (also known as "ghosts X") tending to arrange into (4×6) superlattice are due to excess charge trapped on surface states. Yet another explanation has been proposed by Tsukamoto *et al.*,[11] who constructed a model for the (4×6) surface on the basis of $\zeta(4\times2)$ by Lee *et al.*[1] by triplication of surface unit cell along $\langle110\rangle$ and removal of two out of three surface Ga dimers.

Surface structural models are of basic importance for further studies of surface diffusion, surface chemistry, magnetism, etc. (see, for example, Refs. 12–16). Moreover, recent applications-oriented investigations have shown that the $c(8\times2)/(4\times6)$ GaAs(001) surface has unique and promising properties.[17,18] Since the structure of that surface still does not seem to be ultimately solved, we use noncontact atomic force microscopy technique to verify construction of its top atomic layers.

II. EXPERIMENT

An experimental system consisting of three ultrahigh vacuum (UHV) chambers (preparation, surface analysis, microscope) is used in the experiment. The chambers are interconnected and samples can be prepared and transferred in UHV. The base pressure in the system is 5×10^{-11} mbar. Sample holders can be heated up to 1000 K both in the preparation and in the analysis chambers. The sample is a piece of semi-insulating GaAs epi-ready wafer available commercially (Kelpin Crystals), mounted on a tantalum sheet with metallic gallium as a "glue" to provide sufficient thermal contact between the sample and the holder. The temperature is measured on the sample holder with a thermocouple, and the surface temperature distribution is monitored with an infrared camera. It is expected that, due to significant radiation at 900 K, experimental processing-temperature ranges for different surface reconstructions may differ slightly if different mounting strategy is used.

Scanning microscopy is performed with Park Scientific Instrument VP2 AFM/STM (atomic force microscopy/scanning-tunneling microscopy) apparatus. All data are collected at room temperature, typically within 10–20 h after ion processing of the surface. Atomic force images are obtained in a noncontact (NC-AFM) frequency modulation (FM) mode with the use of a Nanosurf "easyPLL" demodulator. Commercially available piezoresistive silicon noncontact cantilevers are used as probes. The resonant frequencies

of the cantilevers are typically about 200 kHz and the spring constant is 20 N/m. The amplitudes of the cantilevers' oscillations used during the measurements are ~10 nm, and detunings (the detuning is a difference in resonance frequency between the interacting and the free cantilever, which is set by the microcope user) are typically below 200 Hz. Scanning rates are 0.5–2 scanlines per second. Two imaging (sub)modes are used. The first is the topographic mode when the feedback loop alternates the tip-surface distance in order to maintain the constant frequency of the cantilever oscillation. In this case a constant-frequency surface is measured. The second is a "quasi-constant-height" mode more often used for atomically resolved images. In that case the feedback is set very low; consequently, the tip-surface distance is determined by averaging of interaction over many atomic sites and stays almost constant. As a result a frequency shift (Δf) map is measured. In the Δf maps presented here, brighter gray levels indicate larger negative frequency shifts, i.e., stronger attractive interaction. The atomic-scale contrast is due to chemical short-range interactions, which may be attractive or repulsive *in principle*, and which are submerged in a larger attractive and smooth background of mesoscale polarization forces. Therefore, total Δf is always negative and stable operation of the microscope is possible even during the short-range interaction sign switch. Since the collected atomically resolved maps contain constant background, they may be "tuned" with no information loss, in order to expose the investigated features better. In particular, when the surface structure is rough, often only the most protruding atoms are imaged with the constant-height mode, since the short-range interaction vanishes over trenches or valleys. In such a case the zero level of the short-range interaction very likely may be identified on the Δf images with a certain level of gray constituting smooth fields over low parts of the structure. Consequently, atomic-scale objects interacting by attractive and repulsive short-range forces can be identified relative to the zero-level gray, respectively, as the brighter and the darker features.

At the present stage of development of the NC-AFM the stable operation can be achieved in a rather narrow range of scanning parameters (i.e., detuning frequency, oscillation amplitude, strengths of the feedback loops for the tip-surface distance and for the oscillation amplitude), which differs significantly for different surfaces and probes. That imposes serious restrictions on surfaces which can be imaged with atomic resolution by the NC-AFM. First of all, the surfaces cannot have exceedingly modulated electrostatic potential. Next, the surfaces must have large flat parts free from aggregates of excess material, since the scanner tuned to image atomic structures may not be able to pass over such high objects (contact of the tip with the surface usually leads to modification of the atomically sharp tip and often to loss of the resolution). And finally, the surface has to be free from weakly bound adsorbed particles since the scanner may displace or capture such atoms, which inevitably produces very large disturbances of subtle scanner equilibrium.

In order to obtain a surface of sufficient quality, the sample is annealed initially to 800 K for several hours until the vacuum recovers to the low 10^{-10} mbar range. Then, the hot surface (800–900 K) is cleaned with a 0.7 keV Ar^+ beam (~70° off normal) rastered for the dose uniformity, with average ion current density of ~0.5 μA/cm^2. Sputtering cycles of approximately 0.5 h duration are repeated until a chemically clean surface (as checked by AES) and clear LEED pattern are obtained. After termination of sputtering the GaAs sample is cooled down (within ~20 s) by transferring it onto a cold copper block in order to minimize segregation of impurities to the surface.

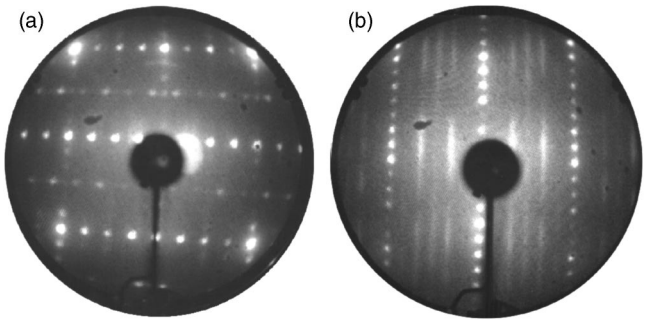

FIG. 1. Low-energy electron diffraction images obtained for GaAs(001) surface; the $c(8\times2)/(4\times6)$ reconstructed surface cleaned at $T=900$ K (a); the (1×6) reconstructed surface obtained at $T=800$ K (b). Electron energy is 36 eV.

III. RESULTS AND DISCUSSION

A. Diffraction studies

Depending on the processing temperature, different surface reconstructions are obtained. If during sputtering the surface temperature is below 850 K, a typical reconstruction is disordered (1×6) [alternatively also referred to as $(n\times6)$ (Ref. 19)]. Around the temperature of 860 K the pseudo (4×6) reconstruction [i.e., a mixture of $c(8\times2)$ and (1×6) domains] is obtained. The $c(8\times2)/(4\times6)$ reconstructed surface can be prepared in a narrow processing temperature window: 870–900 K. Diffraction image of the last surface is shown in Fig. 1(a). As seen, $c(8\times2)$ diffraction spots are dominant but also weak streaking along $\langle 110\rangle$ (vertical direction), and some $(\times6)$ diffraction spots are distinguishable. Of substantial difficulty here is the isolation of the diffraction features arising due to the single $c(8\times2)/(4\times6)$ phase from the secondary pattern arising due to minor (1×6) phase, which is likely to exist close to steps.[16] We believe that this may be accomplished by careful comparison of Fig. 1(a) and 1(b) [the latter displaying the diffraction image of the single (1×6) phase]. It is suggested that the $(\times6)$ diffraction spots close to the brightest (1×1) spots in Fig. 1(a) arise due to the minor (1×6) phase contribution. On the other hand, the weak streaking at $(n/4,1)$ and $(n/4,-1)$ spots, where $n=\pm1,2,3$, is assigned to the single $c(8\times2)/(4\times6)$ phase. It is interesting to note that, in contrast to NC-AFM results (see Sec. III B below), which show the whole surface covered by the disordered (4×6) pattern, the diffraction echo of this pattern is hardly discernible.

B. NC-AFM studies

A large-scale AFM image of $c(8\times2)/(4\times6)$ surface is shown in Fig. 2. The surface is composed of atomically flat

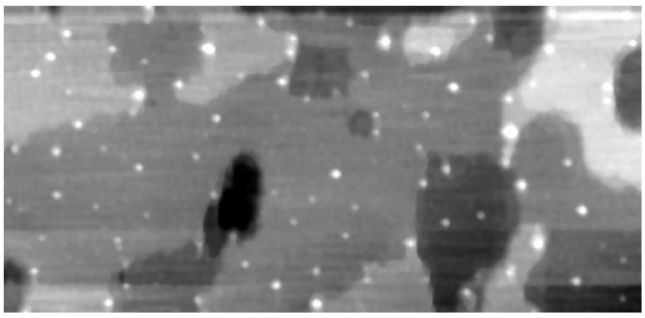

FIG. 2. Overview (500 nm × 250 nm) of sputter-cleaned GaAs surface. The image has been recorded in the topographic mode. Detuning is −18 Hz. Horizontal level is parallel to ⟨110⟩.

terraces of sizes 100–200 nm across. Terrace edges are irregular, likely because of relatively fast sample cooling after termination of sputtering. The typical step height is ~0.2 nm. On the terraces numerous bright spots are seen, by a reasonable assumption being due to excess Ga metal aggregation. Similar bright spots have been seen before on sputter-cleaned $A_{III}B_V$ surfaces (for example, see Ref. 20). Large, up to 100 nm × 100 nm spaces free from the aggregates can be found on the surface for AFM scanning. In Fig. 3 a smaller part of this surface is imaged with high resolution. As seen, at the atomic level the surface is composed of atomic rows running along the ⟨110⟩ crystallographic direction. These rows are crossed by long chains of hazy features running roughly parallell to $\langle\bar{1}10\rangle$. The chains are correlated with each other and often separated by six surface lattice units, although larger separations may be found as well. Doubtless, this is the disordered (4×6) phase (or ghosts X) reported before by several authors. There are also a few surface defects (random bright spots) pictured in the image, which are most probably adsorbates or atomic aggregates. It is interesting to note that along the ⟨110⟩ direction, the phase of the ghost pattern is pinned by these defects.

At this point we would like to discuss mechanisms of FM-NC-AFM contrast formation more extensively, in order to get a better understanding of what in fact is recorded in images obtained using this experimental technique. When the topographic mode is used for large-scale images of chemically uniform (averaged) surfaces the contrast mechanism is

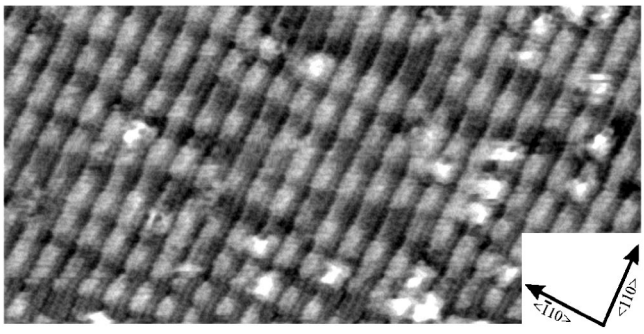

FIG. 3. Δf map of the $c(8\times2/4\times6)$ GaAs surface. Average detuning is −47 Hz; scan rate is 0.8 lines/s. The image size is 40 nm × 20 nm.

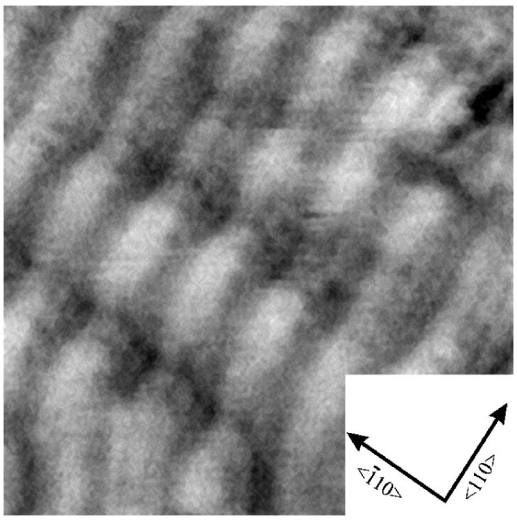

FIG. 4. Δf map of $c(8\times2/4\times6)$ GaAs; average detuning is −18 Hz, scan rate is 2 lines/s. The image size is 10 nm × 10 nm.

simple since, independent of the nature of the tip-surface interaction, the constant frequency envelope is identical to the surface topographic relief. In contrast, for nonuniform surfaces and for atomically resolved images the contrast mechanism is very complex since the cantilever resonant frequency is dependent on a few different components of the tip-surface interaction, i.e.: (i) attractive and long-range, macroscopic electrostatic interaction (ES); (ii) medium-range polarization interaction (often also referred to as the van der Waals or vdW interaction), and (iii) short-range chemical interaction (CH), which may also include microscopic electrostatic forces. Atomic pattern can be resolved thanks to CH operating around the cantilever lower turning point. In order to obtain atomically resolved images on conductive samples, it is necessary to cancel extremely large and long-ranged ES capacitance forces. This is done by applying a constant bias voltage between the tip and the sample, which is determined by minimizing the average ES interaction. If large mesoscopic inhomogeneities of the surface electrostatic potential are present, their pattern will be visible in NC-AFM images and may even completely dominate the contrast.[21,22] The chemical interaction term is strongly dependent on the tip-front morphology. It is believed that intense atomic-scale contrast is seen on semiconductor surfaces when the tip is terminated with a stable single atom interacting by covalent forces with surface atoms,[23,24] although microscopic electrostatic forces have been reported to come into play as well.[25] Fortunately, since different interactions have different ranges, by tuning the tip-surface distance (i.e., average frequency shift), one may change their relative contributions to the NC-AFM image contrast, and often it is even possible to obtain separate images dominated by one kind of interaction.[26,27]

In order to disclose the nature of ghosts X, images recorded at lower and higher detunings, referring to the one applied for the map in Fig. 3, are shown. In Fig. 4 the Δf the image of "far" interactions, i.e., obtained with low detuning, is presented. Since atomic features (i.e., ones of sizes less than 0.5 nm) can hardly be seen, it is apparent that the mi-

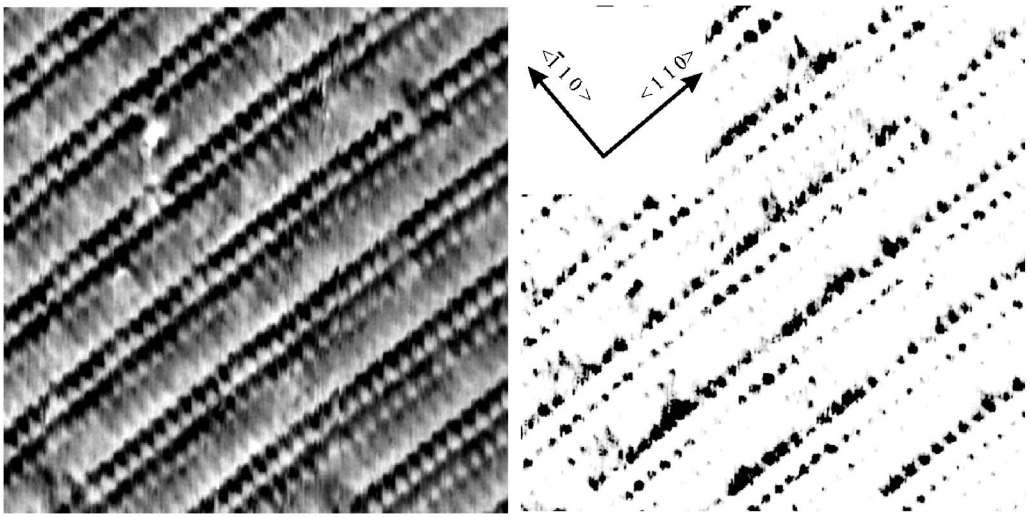

FIG. 5. Left panel: Δf map of $c(8\times2/4\times6)$ GaAs; average detuning is −136 Hz, scan rate is 2 lines/s. The image size is 10 nm×10 nm. Right panel: the same map overcontrasted to evidence modulation of intensity along atomic rows.

croscope operates beyond the chemical interaction range and consequently the observed pattern arises due to modulation of the electrostatic field alone. The pattern, which is explicitly formed by the ghosts X, evidences the intimate relation between the ghosts and the surface charge density distribution. Although it is anticipated that metallic clusters on semiconductor surface would not be electrically neutral and could generate far images similar to the one seen in Fig. 4, this hypothesis has to be dismissed in view of the "close" Δf map, which is obtained using high detuning and has its contrast dominated by short-range interactions (cf. Fig. 5). The latter map displays only sharp, atomic-scale features distributed on the (4×1) lattice. In more detail the close pattern is comprised of triple rows of bright spots running parallel to $\langle110\rangle$ containing also intense dark spots between the bright ones. At careful inspection, traces of ghosts X may be noticed in Fig. 5 only as slight modulation in intensity of certain atomic features along the $\langle110\rangle$ direction. Thus, it is evidenced that neither clusters of excess material[5] nor surface dimers distributed with $(\times6)$ period[11] can be implemented to account for the disordered (4×6) reconstruction of GaAs(001) surface.

C. The $\zeta c(8\times2)$ model and NC-AFM maps

The ζ model is a universal description of $c(8\times2)$ reconstructed surfaces of $A_{III}B_V$ compounds. It has been proposed independently by Lee *et al.* (Ref. 1) on the basis of total energy calculations and by Kumpf *et al.* (Ref. 2) on the basis of surface x-ray diffraction (SXRD), supported by the direct methods for surface structure determination. Differences in surfaces of different compounds are explained by different occupancies of certain surface lattice sites within the same general model. According to Lee *et al.* the top bilayer of GaAs(001) is built of (4×2) structural units, where a double period along $\langle110\rangle$ arises due to dimerization of surface Ga atoms. The $c(8\times2)$ reconstruction is stabilized by dimers of A_{III} atoms arranged to form a $c(8\times2)$ network buried in the second bilayer. Real GaAs surface reconstructed from SXRD data by Kumpf *et al.* is described basically by the same lattice but is partially disordered, i.e., it has stochastic fractional occupancies of certain surface sites. For example, only 63% of surface Ga dimers are present and the remaining 37% of the dimer sites are vacant.

Real-space images may be of crucial importance for surface structure investigation[28] but, on the other hand, when the atomic-scale features are interpreted with no sufficient criticism they also may be misleading, which is best illustrated by the case of InSb(001) $c(8\times2)$ surface structure investigation with scanning-tunneling microscopy technique.[29,30] According to Hove, perhaps even half of published STM images of all other surfaces have been incorrectly interpreted because of assignment of bumps and protrusions simply as atoms.[31] The problem is, however, more general, i.e., not limited to the STM technique, and given the complex NC-AFM contrast mechanisms, simple interpretation of NC-AFM images would probably be similarly hazardous. However, while direct identification of atomic-scale features may be unsure, reliable information about surface symmetry, domains, degree of disorder, and surface defects is readily available from scanning-probe images. Therefore, results obtained either by STM or NC-AFM may be safely used for tests of existing structural models, or as starting data for surface-structure iterations.

There is unavoidable ambiguity in the NC-AFM data resulting from the fact that the type of the tip-front atom and its orientation are not known (the same obviously applies for STM). During the NC-AFM experiment the tip sometimes suffers accidental contact with the surface, and the tip-front configuration may change. Intentional crashes of the tip on the probed surface are often used as a way to modify morphology of the tip apex when it is not providing adequate contrast. However, in most cases the tip-front atom is, by reasonable assumption, either the constituent of the tip, or the constituent of the surface. Recently, the problem of NC-AFM imaging in the context of different tip morphologies has been evaluated by Tobik *et al.* and Ke *et al.*,[23,24] who

used the density functional theory to calculate the chemical interaction of silicon tip with surfaces of $A_{III}B_V$ compounds. They considered three of the most probable tip configurations, i.e. (1) The A_{III} atom terminated tip with an empty dangling bond sticking out to the surface; (2) the B_V atom terminated tip with a fully filled dangling bond; and (3) the Si atom terminated tip with a half-filled dangling bond. The general conclusion is that, due to interactions between differently occupied dangling bonds of the tip and of the surface, the tips (1), (2), and (3) should generate images of B_V sublattice, A_{III} sublattice, and composite A_{III} and B_V sublattice, respectively. Those results have been obtained for the (011) surfaces of GaAs and InP. However, due to the calculation methods used, it is not expected that the general trends would change appreciably by looking at a different crystal face or by considering a more complex tip termination preserving the same basic chemistry.[32] NC-AFM ability to image $A_{III}B_V$ sublattices separately has been confirmed recently on the InSb $c(8\times2)$ surface.[3] This gives hope that the atomic-scale features seen by the NC-AFM on $A_{III}B_V$ surfaces can be, in most cases (i.e., when the tip is terminated by a single atom), interpreted cautiously as atoms. One has to keep in mind, however, that with the Δf scanning mode, the atoms in trenches will not be resolved since the chemical interaction is of short range, and that (within the CH interaction range) the elevation of atoms in different chemical configurations may not be reflected monotonically with the brightness of the corresponding features, since the NC-AFM contrast is due to a convolution of the geometric and chemical factors, and additionally it may be influenced by local elastic properties (stretching or compression) of the imaged structure.[33]

Atomically resolved patterns obtained for the investigated surface display prevailing (4×1) surface symmetry, evidence single phase, and show no atomic disorder in the strict surface layer. As an attempt to identify atomic-scale features seen on the NC-AFM Δf map of GaAs surface in a context of the recent $\zeta c(8\times2)$ model, a part of the map shown in Fig. 5 has been magnified and the surface unit cell obtained from the ζ model (but with no surface dimers) has been overlaid on the map. The result is shown in Fig. 6. Our analysis is started with the identification of a double row of dark spots, which we assign as the type As6 atoms interacting with the tip in a repulsive mode (either by the chemical- or by the core-core interactions). Next, we assign the middle row of bright spots as Ga2 and Ga3 atoms and the side rows as Ga4 and Ga5 atoms interacting in an attractive mode. Then, we find that the Ga1 atoms are missing, which is consistent with previous results,[1,2] and that the As7 and As8 atoms in trenches are not resolved as expected [cf. Ref. 2 for a detailed description of atom types in the $\zeta c(8\times2)$ lattice]. Also, it is worth noting that the gray level of smooth fields representing trenches (about the missing Ga1 sites) reflects the cantilever resonant frequency corresponding approximately to the zero level of the short-range interaction. This is a rationale for our assignment of dark features seen in Fig. 6 as corresponding to repulsive short-range interactions. Since we find a very striking consistency between our maps and the ζ model, we finally conclude that the bright pattern seen in Figs. 5 and 6 reproduces the Ga sublattice of $\zeta c(8\times2)$ GaAs(001) surface layer. Interestingly, neither surface dimers in the Ga2/Ga3 row as proposed by Lee *et al.*[1] nor partial occupancies in the same row as proposed by Kumpf *et al.*[2] can be seen.

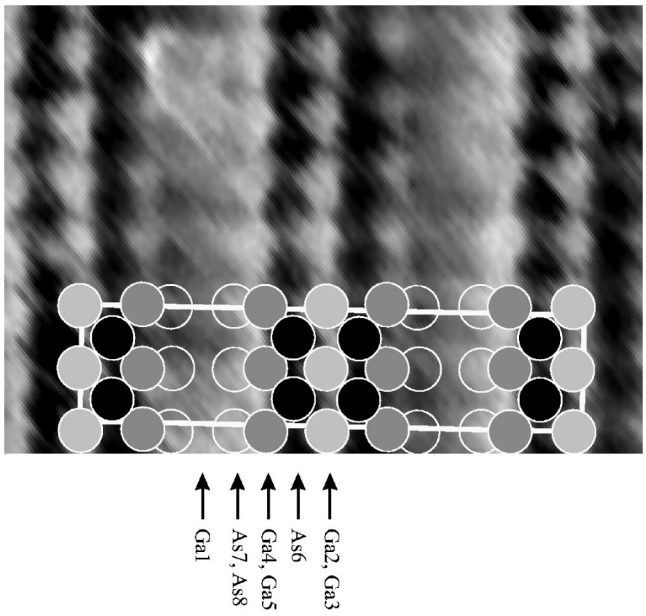

FIG. 6. Part of the map in Fig. 5 ($\sim$4 nm$\times$2.8 nm) with overlaid surface unit cell conforming to the $\zeta c(8\times2)$ model. Arrows show the types of atoms in the ζ model; "high" and "low" atoms are indicated, respectively, by filled and empty circles. Location of the missing row of Ga1-type atoms, which is the most protruding row in the model, is marked also. See Ref. 2 for details of the ζ model. The image is rotated in order to align the $\langle110\rangle$ direction vertically.

D. What are the ghosts X?

A literature survey[5,7–9,11,34] indicates that very likely the ghosts X are inherent in the $c(8\times2)$ GaAs(001) surface prepared at high temperature and at low-arsenic conditions. It is also anticipated that the surface analyzed with SXRD by Kumpf *et al.* could contain the ghosts X since a disorder in the surface has been reported, and the preparation procedure[35] used [i.e., evaporation of arsenic protective layer from the MBE-grown GaAs(001) surfaces followed by thermal annealing] is known to yield $c(8\times2)$ surface with ghosts.[7] Taking into account the above and the similarities between the ζ model and the $c(8\times2)$ surface geometry obtained by NC-AFM (see Sec. III C), it seems quite straightforward that the ζ model should constitute a starting point for developing a detailed picture of the surface structure under discussion. It is evidenced by the NC-AFM images shown above that neither the concept of additional objects (for example, gallium aggregates) distributed on the surface nor the concept of disorder in the strict surface layer (missing dimers, atoms, etc.) can be used to explain the $c(8\times2)/(4\times6)$ surface reconstruction of GaAs(001). The concept which cannot be excluded directly on grounds of NC-AFM experiment is that of additional subsurface reconstruction superimposed on the ζ structure. However, having in mind the

very weak LEED echo of the ghosts, we point out that there is probably no significant difference between the pure $c(8\times2)$ structure and the $c(8\times2)/(4\times6)$ one, as far as positions of atomic cores are concerned. Consequently, we conclude, in agreement with views of Kruse *et al.* (Ref. 7), that the ghosts X are due to specific surface electronic states. Such states could cause the modulation of surface electrostatic potential, but with no significant effect on LEED patterns at electron energies above 30 eV.[36] Visible streaking in the patterns could be possible, however, due to small secondary shifts of atomic positions in partially ionic-solid surface, following the in-plane electric field. Because of these distortions, it is also anticipated that the surface structures derived from analysis of SXRD data may be, to some extent, inaccurate since many $c(8\times2)$ and (4×6) diffraction reflexes have to interfere. In particular, the partial occupancies of the ζ model sites reported in Ref. 2, but not confirmed in the present study, might be caused by not taking into account the ghost pattern superimposed on the $c(8\times2)$ surface, although we must admit that there is no way to completely exclude the possibility that these differences are real and caused by different surface preparation procedures.[37]

Finally, we would like to remark that at solid surfaces with strong anisotropy, such as $c(8\times2)$ GaAs(001), exotic electronic states related to reduced dimensionality are likely.[38–40] Such states often show a non-Fermi liquid character and induce periodic spatial modulation of surface charge density, i.e., charge density wave (CDW). Spectroscopic studies are necessary to investigate the possible metallicity and details of the electronic structure of the $c(8\times2)/(4\times6)$ GaAs(001) surface, in order to disclose the nature of the observed surface CDW. We would like to point out also that the idea of the CDW quantum state seems particularly attractive in the context of surfaces investigated here, since it would readily explain the different stages of disorder found in the ghost pattern by different authors, as the phase of the CDW pattern is often pinned to extrinsic structural defects,[41,42] while the density of surface defects critically depends on surface preparation procedure. Moreover, characteristic phase pinning of the ghost pattern by randomly distributed surface defects is clearly observed in our NC-AFM images (see Fig. 3).

IV. CONCLUSIONS

In conclusion, we have studied surface structure of $c(8\times2)/(4\times6)$ GaAs(001) surface using the frequency-modulated NC-AFM technique. It has been found that the surface is covered with mysterious features (ghosts X), which are aligned in chains along $\langle\overline{1}10\rangle$ and partially disordered but tending towards $(\times6)$ period along the $\langle110\rangle$ direction.

The atomically resolved images, which have their contrast dominated by short-range interactions, indicate that the strict surface layer has the (4×1) symmetry and its surface unit cell seems to be well described with the recent revolutionary ζ model. However, neither additional atomic clusters nor missing atoms or dimers are observed in correlation with the ghosts X. Therefore, we indicate that the ghosts X have no material nature and they are visible due to spatially modulated electrostatic potential induced by surface charge density wave.

Although a harmony between the ζ model and NC-AFM atomic pattern is unquestionable, the detailed structure of the surface appears somewhat different from earlier suggestions. In particular, neither surface dimers nor partial occupancies of certain surface sites have been found. Having in mind recent misinterpretations of STM images for A_{III}-rich surfaces of $A_{III}B_V$ compounds, we prefer not to make a categorical statement about the structure of $c(8\times2)/(4\times6)$ GaAs surface. Nevertheless, we would like to stress that on the basis of NC-AFM experiment, the single-ζ phase with a charge density wave is presently the most coherent description of this surface prepared at high temperature and at low-arsenic conditions.

ACKNOWLEDGMENT

The present work has been supported by the Polish Committee for Scientific Research under Project No. 1P03B 067 26.

*Electronic address: jkolodz@if.uj.edu.pl

[1] S.-H. Lee, W. Moritz, and M. Scheffler, Phys. Rev. Lett. **85**, 3890 (2000).

[2] C. Kumpf, L. D. Marks, D. Ellis, D. Smilgies, E. Landemark, M. Nielsen, R. Feidenhans'l, J. Zegenhagen, O. Bunk, J. H. Zeysing, Y. Su, and R. L. Johnson, Phys. Rev. Lett. **86**, 3586 (2001).

[3] J. J. Kolodziej, B. Such, M. Szymonski, and F. Krok, Phys. Rev. Lett. **90**, 226101 (2003).

[4] T. D. Mishima, N. Naruse, S. P. Cho, T. Kadohira, and T. Osaka, Phys. Rev. Lett. **89**, 276105 (2002).

[5] Q. Xue, T. Hashimizu, J. M. Zhou, T. Sakata, T. Ohno, and T. Sakurai, Phys. Rev. Lett. **74**, 3177 (1995).

[6] Diffraction spots in LEED images of GaAs surfaces processed at temperatures close to 900 K often show streaking along half-order rows, which has been assigned to the mixture of $c(8\times2)$ and (4×2) phases, which consist of identical structural (4×2) subunits, most probably by analogy to the $c(2\times8)/(2\times4)$ GaAs phase. On the other hand, microscopic studies as a rule show only (4×1) symmetry on that surface. Depending on the characterization technique and the preparation method used, different authors use different Wood's reconstruction symbols likely for the same general surface structure.

[7] P. Kruse, J. G. McLean, and A. C. Kummel, J. Chem. Phys. **113**, 2060 (2000).

[8] R. Moosbuehler, F. Bensch, M. Dumm, and G. Bayreuther, J. Appl. Phys. **91**, 8757 (2002).

[9] N. Negoro, S. Anantathansarn, and H. Hasegawa, J. Vac. Sci. Technol. B **21**, 1945 (2003).
[10] Q.-K. Xu, T. Hahimizu, and T. Sakurai, Appl. Surf. Sci. **141**, 244 (1999).
[11] S. Tsukamoto, M. Pristovsek, A. Ohtake, B. G. Orr, G. R. Bell, T. Ohno, and N. Koguchi, J. Cryst. Growth **251**, 46 (2003).
[12] W. C. Simpson, D. K. Shuh, W. H. Hung, J. Vac. Sci. Technol. A **14**, 1815 (1996).
[13] A. Kley, P. Ruggerone, and M. Scheffler, Phys. Rev. Lett. **79**, 5278 (1997).
[14] T. Zhang, N. Takahashi, M. Spangenberg, T.-H. Shen, E. A. Seddon, D. Greig, and J. A. D. Matthew, Appl. Surf. Sci. **193**, 217 (2002).
[15] Q. Fu, L. Li, M. J. Begarney, D. C. Law, and R. F. Hickset, J. Phys. Chem. B, **104**, 5595 (2000).
[16] J. G. McLean, P. Kruse, J. Guo-Ping, H. E. Ruda, and A. C. Kummel, Phys. Rev. Lett. **85**, 1488 (2000).
[17] H. Yamaguchi, K. Kanisawa, and Y. Horikoshi, Phys. Rev. B **53**, 7880 (1996).
[18] S. Anantathanasarn and H. Hasegawa, Appl. Surf. Sci. **216**, 275 (2003).
[19] B. Such, J. J. Kolodziej, P. Czuba, F. Krok, P. Piatkowski, P. Struski, and M. Szymonski, Surf. Sci. **530**, 149 (2003).
[20] C. F. McConville, T. S. Jones, F. M. Leibsle, S. M. Driver, T. C. Q. Noakes, M. O. Schweitzer, and N. V. Richardson, Phys. Rev. B **50**, 14 965 (1994).
[21] We have made several unsuccessful attempts to image GaAs surface with NC-AFM as only structureless and very rough images have been seen, despite the fact that LEED produced a very sharp (4×1) pattern. Since the samples used were cut out from heavy-doped wafers and postannealed, the problem was most probably associated with segregation of electrically active Si dopants to the surface, which caused excessive folding of surface electrostatic potential in a mesoscale.
[22] A. Schwarz, W. Allers, U. D. Schwarz, and R. Wiesendanger, Phys. Rev. B **62**, 13 617 (2000).
[23] J. Tobik, I. Stich, and K. Terakura, Phys. Rev. B **63**, 245324 (2001).
[24] S. H. Ke, T. Uda, I. Stich, and K. Terakura, Phys. Rev. B **63**, 245323 (2001).
[25] M. Guggisberg, O. Pfeiffer, S. Schaar, M. Bamerlin, Ch. Loppacher, R. Benewitz, A. Baratoff, and E. Meyer, Appl. Phys. A: Mater. Sci. Process. **72**, S19 (2001).
[26] M. Guggisberg, M. Bammerlin, Ch. Loppacher, O. Pfeiffer, A. Abdurixit, V. Barwich, R. Bennewitz, A. Baratoff, E. Meyer, and H. J. Guntherodt, Phys. Rev. B **61**, 11 151 (2000).
[27] R. Nishii, S. Araragi, K. Shirai, Y. Sugawara, and S. Morita, Appl. Surf. Sci. **210**, 90 (2003).
[28] G. Binnig, H. Rohrer, C. Gerber, and E. Weibel, Phys. Rev. Lett. **50**, 120 (1983).
[29] M. O. Schweitzer, F. M. Leibsle, T. S. Jones, C. F. McConville, and N. V. Richardson, Surf. Sci. **280**, 63 (1993).
[30] A. A. Davis, R. G. Jones, G. Falkenberg, L. Seehofer, R. L. Johnson, and C. F. McConville, Appl. Phys. Lett. **75**, 1938 (1999).
[31] M. A. van Hove, Surf. Interface Anal. **28**, 36 (1999).
[32] I. Stich (private communication).
[33] R. Bennewitz, A. S. Foster, L. N. Kantorovich, M. Bammerlin, C. Loppacher, S. Schaar, M. Guggisberg, E. Meyer, and A. S. Schluger, Phys. Rev. B **62**, 2074 (2000).
[34] P. Kocán, A. Ohtake, and N. Koguchi, Phys. Rev. B **70**, 201303 (2004).
[35] U. Resch-Esser, N. Esser, D. T. Wang, M. Kuball, J. Zegenhagen, B. O. Fimland, M. Cardona, and W. Richter, Surf. Sci. **352-354**, 71 (1996).
[36] M. A. van Hove, W. H. Weinberg, and C.-M. Chan, *Low Energy Electron Diffraction*, edited by G. Ertl (Springer-Verlag, Berlin, 1986), pp. 188–189.
[37] In the course of a literature survey concerning Ga-rich GaAs surfaces, we noticed that LEED diffraction patterns of these surfaces are rarely published. This often makes the direct comparisons difficult since, even for sputter-cleaned GaAs(001), there are many differently reconstructed surfaces observed. Apart from the ones discussed in the paper, incidentally we also saw (4×1), streaky (4×2), (4×3), (3×2), as well as mixed and faceted surfaces. With insufficient attention paid to surface temperature distribution, different reconstructions existed simultaneously on different parts of the sample. Some of those reconstructions might be related to adsorbates, and some to segregation of bulk impurities since they were observed after prolonged postannealing of Si-doped samples. Of course, one can compare scanning-probe real-space images if available, but this is straightforward only in the positive case, i.e., when the images show the same structure. In the negative case, i.e., when the images are different, the result of the comparison is ambiguous since the differences may be caused by different tip termination, different sample bias, or both.
[38] J. M. Carpinelli, H. H. Weitering, M. Bartkowiak, E. W. Plummer, and R. Stumpf, Nature (London) **381**, 398 (1996).
[39] J. M. Carpinelli, H. H. Weitering, M. Bartkowiak, R. Stumpf, and E. W. Plummer, Phys. Rev. Lett. **79**, 2859 (1997).
[40] H. W. Yeom, S. Takeda, E. Rotenberg, I. Matsuda, K. Horikoshi, J. Schaefer, C. M. Lee, S. D. Kevan, T. Ohta, T. Nagao, and S. Hasegawa, Phys. Rev. Lett. **82**, 4898 (1999).
[41] A. V. Melechko, J. Braun, H. H. Weitering, and E. W. Plummer, Phys. Rev. Lett. **83**, 999 (1999), Phys. Rev. B **61**, 2235 (2000).
[42] S. S. Lee, J. R. Ahn, N. D. Kim, J. H. Min, C. G. Hwang, J. W. Chung, H. W. Yeom, S. V. Ryjkov, and S. Hasegawa, Phys. Rev. Lett. **88**, 196401 (2002).